Enhancement of the Ion-Transport Selectivity of Layered Polyelectrolyte Membranes through Cross-Linking and Hybridization

Jacqueline L. Stair, Jeremy J. Harris, and Merlin L. Bruening*

Department of Chemistry, Michigan State University, East Lansing, Michigan 48824

Received February 9, 2001. Revised Manuscript Received June 4, 2001

Layer-by-layer deposition of polyelectrolytes on porous supports is a convenient method for producing ultrathin membranes with moderate ion-transport selectivities. This study shows that the capping of poly(styrene sulfonate) (PSS)/poly(allylamine hydrochloride) (PAH) membranes with a few layer pairs of poly(acrylic acid) (PAA)/PAH results in dramatic increases in anion-transport selectivity. Deposition of less than eight total layer pairs yields reliable Cl^-/SO_4^{2-} and $Cl^-/Fe(CN)_6^{3-}$ selectivities up to 150 and 3000, respectively. Field-emission scanning electron microscope images show that the surface structure of PAA/PAH is altered by deposition on PSS/PAH, and we surmise that the PAA/PAH on these hybrid films is less strongly hydrated than the surface of pure PAA/PAH membranes. This would result in a higher surface charge density and more Donnan exclusion of multiply charged ions. Termination of membranes with PAH rather than PAA greatly reduces (in some cases reverses) Cl^-/SO_4^{2-} selectivities, demonstrating that selectivity is indeed largely due to Donnan exclusion at the membrane surface. Cross-linking of pure PAA/PAH membranes through heat-induced amidation can increase Cl^-/SO_4^{2-} selectivity as much as 4-fold. Because of their minimal thicknesses, hybrid polyelectrolyte films can be selective without greatly hindering the flux of monovalent ions. Thus, these films are attractive for applications such as water softening.

Introduction

Alternating deposition of polycations and polyanions on porous supports is an extremely versatile method for synthesizing thin separation membranes.[1−3] However, the gas or ion selectivity of these membranes is usually modest unless many layers are deposited on the support.[4−11] In this paper, we show that deposition of one to three capping bilayers[12] of poly(acrylic acid) (PAA)/poly(allylamine hydrochloride) (PAH) on top of five bilayers of poly(styrene sulfonate) (PSS)/PAH yields remarkable (up to 30-fold) increases in anion-transport selectivities. Cross-linking of PAA/PAH films also enhances transport selectivity. The high monovalent/divalent ion selectivity of these membranes makes them attractive candidates for water purification.

Separation of monovalent and divalent ions in solution is an important part of applications such as water softening,[13,14] purification of groundwater,[15−19] and production of edible and raw salt from seawater.[20] For example, reductions in SO_4^{2-} concentrations allow for human consumption of salt produced from seawater and prevent scaling of membranes and seawater reservoirs through precipitation of compounds such as $CaSO_4$.[20,21] Although membranes are available for such applications, increased ion selectivity will make these processes much more effective.

Many ion-separation membranes consist of ion-exchange materials that exhibit moderate selectivities among either cations or anions.[22−27] Specific modifica-

* Author to whom correspondence should be addressed. E-mail: bruening@cem.msu.edu. Phone: (517) 355-9715 ext. 237. Fax: (517) 353-1793.

(1) Decher, G.; Hong, J. D. *Ber. Bunsen-Ges. Phys. Chem.* **1991**, *95*, 1430.
(2) Decher, G.; Hong, J. D.; Schmitt, J. *Thin Solid Films* **1992**, *210/211*, 831.
(3) Decher, G. *Science* **1997**, *277*, 1232.
(4) Stroeve, P.; Vasquez, V.; Coelho, M. A. N.; Rabolt, J. F. *Thin Solid Films* **1996**, *284−285*, 708.
(5) Leväsalmi, J.-M.; McCarthy, T. J. *Macromolecules* **1997**, *30*, 1752.
(6) Krasemann, L.; Tieke, B. *Langmuir* **2000**, *16*, 287.
(7) Krasemann, L.; Tieke, B. *Mater. Sci. Eng. C* **1999**, *8−9*, 513.
(8) Krasemann, L.; Tieke, B. *J. Membr. Sci.* **1998**, *150*, 23.
(9) van Ackern, F.; Krasemann, L.; Tieke, B. *Thin Solid Films* **1998**, *327−329*, 762.
(10) Quinn, R.; Laciak, D. V. *J. Membr. Sci.* **1997**, *131*, 49.
(11) Zhou, P.; Samuelson, L.; Alva, K. S.; Chen, C.-C.; Blumstein, R. B.; Blumstein, A. *Macromolecules* **1997**, *30*, 1577.
(12) There is substantial interpenetration between alternating layers of polyelectrolytes; thus, the terms "bilayer" and "layer" are used loosely. (See refs 3 and 35.)
(13) Brett, S. W.; Gaterell, M. R.; Morse, G. K.; Lester, J. N. *Environ. Technol.* **1999**, *20*, 1009.
(14) Mika, A. M.; Childs, R. F.; Dickson, J. M. *Desalination* **1999**, *121*, 149.
(15) Bader, M. S. H. *J. Hazard. Mater.* **2000**, *B73*, 269.
(16) Amor, Z.; Malki, S.; Taky, M.; Bariou, B.; Mameri, N.; Elmidaoui, A. *Desalination* **1998**, *120*, 263.
(17) Hell, F.; Lahnsteiner, J.; Frischherz, H.; Baumgartner, G. *Desalination* **1998**, *117*, 173.
(18) Sata, T.; Yamaguchi, T.; Matsusaki, K. *J. Chem. Soc., Chem. Commun.* **1995**, 1153.
(19) Oldani, M.; Killer, E.; Miquel, A.; Schock, G. *J. Membr. Sci.* **1992**, *75*, 265.
(20) Saracco, G.; Zanetti, M. C. *Ind. Eng. Chem. Res.* **1994**, *33*, 96.
(21) Sata, T.; Mine, K.; Higa, M. *J. Membr. Sci.* **1998**, *141*, 137.
(22) Sata, T. *J. Membr. Sci.* **2000**, *167*, 1.
(23) Mizutani, Y. *J. Membr. Sci.* **1990**, *54*, 233.

10.1021/cm010166e CCC: $20.00
Published on Web 07/11/2001

tions of these membranes designed to increase selectivity include deposition of a highly charged surface layer,[28,29] cross-linking of the membranes' interiors,[30] and incorporation of hydrophobic/hydrophilic groups within the film and on the surface.[25,31,32] Selective transport through these films is based on anion size, charge, hydration energy, and specific chemical interactions with the membranes.

Layered polyelectrolyte films are especially attractive membrane materials because of their ease of deposition and wide variability. The minimal thickness of these films should also allow for high fluxes. Deposition of layered polyelectrolyte films, first demonstrated by Decher and co-workers,[1] simply involves the alternating adsorption of polycations and polyanions to form multilayer assemblies held together by electrostatic interactions. Recently, Schlenoff and co-workers showed that this process can be performed by sequential spraying of polyelectrolytes onto desired substrates.[33] Film buildup occurs by charge overcompensation,[34−36] which provides coverage of defects and inhomogenities in previous layers.[3,37,38] This mechanism also allows for the formation of composite membranes through the coverage of porous supports with defect-free films.[39] Significantly, polyelectrolyte deposition occurs from aqueous solutions, rendering this procedure more environmentally friendly than most film-formation techniques.

The versatility of alternating polyelectrolyte deposition is evident from the large number of substrates and polyelectrolytes that can be used to form these films.[40−47] Synthesis can occur on most charged or polar[43,48] substrates, as well as some polymer substrates,[4,43,49−51] and is independent of substrate size and topology.[1,2] Materials capable of forming layered polyelectrolyte films include dendrimers,[52−54] proteins,[45,55−59] alumosilicates,[60,61] nucleic acids,[62−64] conducting polymers,[55,65−67] semiconductor nanoparticles,[68] dyes,[40,48] light-emitting molecules,[69] and inorganic ions.[70] This variety of materials should afford control over selective permeation through these films. Additionally, alteration of deposition parameters (i.e., pH,[71−75] polymer concentration,[76] number of bilayers,[77] supporting salt concentration,[37,71,78−82] and drying procedures[37,83]) allows for the tailoring of film characteristics such as thickness, density, charge density, and pore size.

One means of utilizing polyelectrolytes for membrane modification is deposition of a single layer of polyelectrolyte to modify an existing membrane.[28,84−86] Tsuru

(24) Sata, T.; Kawamura, K. *J. Membr. Sci.* **2000**, *171*, 97.
(25) Eyal, A.; Kedem, O. *J. Membr. Sci.* **1988**, *38*, 101.
(26) Sata, T. *J. Membr. Sci.* **1994**, *93*, 117.
(27) Andrés, L. J.; Riera, F. A.; Alvarez, R.; Audinos, R. *Can. J. Chem. Eng.* **1994**, *72*, 848.
(28) Takata, K.; Yamamoto, Y.; Sata, T. *J. Membr. Sci.* **2000**, *179*, 101.
(29) Takata, K.; Yamamoto, Y.; Sata, T. *Bull. Chem. Soc. Jpn.* **1996**, *69*, 797.
(30) Sata, T.; Nojima, S. *J. Polym. Sci. B: Polym. Phys.* **1999**, *37*, 1773.
(31) Sata, T.; Shimokawa, Y.; Matsusaki, K. *J. Membr. Sci.* **2000**, *171*, 31.
(32) Sata, T.; Yamaguchi, T.; Matsusaki, K. *J. Phys. Chem.* **1996**, *100*, 16633.
(33) Schlenoff, J. B.; Dubas, S. T.; Farhat, T. R. *Langmuir* **2000**, *16*, 9968.
(34) Caruso, F.; Donath, E.; Möhwald, H. *J. Phys. Chem. B* **1998**, *102*, 2011.
(35) Schlenoff, J. B.; Ly, H.; Li, M. *J. Am. Chem. Soc.* **1998**, *120*, 7626.
(36) Joanny, J. F. *Eur. Phys. J. B* **1999**, *9*, 117.
(37) Ladam, G.; Schaad, P.; Voegel, J. C.; Schaaf, P.; Decher, G.; Cuisiner, F. *Langmuir* **2000**, *16*, 1249.
(38) Ramsden, J. J. *Thin Solid Films* **1995**, *254*, 246.
(39) Harris, J. J.; Stair, J. L.; Bruening, M. L. *Chem. Mater.* **2000**, *12*, 1941.
(40) von Klitzing, R.; Möhwald, H. *Thin Solid Films* **1996**, *284−285*, 352.
(41) Han, S.; Lindholm-Sethson, B. *Electrochim. Acta* **1999**, *45*, 845.
(42) Ichinose, I.; Mizuki, S.; Ohno, S.; Shiraishi, H.; Kunitake, T. *Polym. J.* **1999**, *31*, 1065.
(43) Delcorte, A.; Bertrand, P.; Wischerhoff, E.; Laschewsky, A. *Langmuir* **1997**, *13*, 5125.
(44) Möhwald, H. *Colloids Surf. A: Physicochem. Eng. Aspects* **2000**, *171*, 25.
(45) Lvov, Y.; Ariga, K.; Ichinose, I.; Kunitake, T. *J. Am. Chem. Soc.* **1995**, *117*, 6117.
(46) Russell, R. J.; Sirkar, K.; Pishko, M. V. *Langmuir* **2000**, *16*, 4052.
(47) Caruso, F.; Niikura, K.; Furlong, D. N.; Okahata, Y. *Langmuir* **1997**, *13*, 3422.
(48) Laschewsky, A.; Wischerhoff, E.; Kauranen, M.; Persoons, A. *Macromolecules* **1997**, *30*, 8304.
(49) Phuvanartnuruks, V.; McCarthy, T. J. *Macromolecules* **1998**, *31*, 1, 1906.
(50) Hsieh, M. C.; Farris, R. J.; McCarthy, T. J. *Macromolecules* **1997**, *30*, 8453.
(51) Fadeev, A. Y.; McCarthy, T. J. *Langmuir* **1998**, *14*, 5586.
(52) Watanabe, S.; Regen, S. L. *J. Am. Chem. Soc.* **1994**, *116*, 8855.
(53) Tsukruk, V. V.; Rinderspacher, F.; Bliznyuk, V. N. *Langmuir* **1997**, *13*, 2171.
(54) Tsukruk, V. V. *Adv. Mater.* **1998**, *10*, 253.
(55) Kotov, N. A.; Haraszti, T.; Turi, L.; Zavala, G.; Geer, R.; Dékány, I.; Fendler, J. H. *J. Am. Chem. Soc.* **1997**, *119*, 6821.
(56) Lvov, Y.; Haas, H.; Decher, G.; Möhwald, H.; Mikhailov, A.; Mtchedlishvily, B.; Morgunova, E.; Vainstein, B. *Langmuir* **1994**, *10*, 4232.
(57) Onda, M.; Lvov, Y.; Ariga, K.; Kunitake, T. *Biotechnol. Bioeng.* **1996**, 51.
(58) Hodak, J.; Etchenique, R.; Calvo, E.; Singhal, K.; Bartlett, P. N. *Langmuir* **1997**, *13*, 2708.
(59) Caruso, F.; Niikura, K.; Furlong, N.; Okahata, Y. *Langmuir* **1997**, *13*, 3427.
(60) Kotov, N. A.; Magonov, S.; Tropsha, E. *Chem. Mater.* **1998**, *10*, 886.
(61) Lvov, Y.; Ariga, K.; Ichinose, I.; Kunitake, T. *Langmuir* **1996**, *12*, 3038.
(62) Montrel, M. M.; Sukhorukov, G. B.; Shabarchina, L. I.; Apolonnik, N. V.; Sukhorukov, B. I. *Mater. Sci. Eng. C* **1998**, *5*, 275.
(63) Lvov, Y. M.; Zhongqing, L.; Schenkman, J. B.; Xiaolin, Z.; Rusling, J. F. *J. Am. Chem. Soc.* **1998**, *120*, 4073.
(64) Lvov, Y.; Decher, G.; Sukhorukov, G. *Macromolecules* **1993**, *26*, 5396.
(65) Fou, A. C.; Rubner, M. F. *Macromolecules* **1995**, *28*, 7115.
(66) Cheung, J. H.; Fou, A. F.; Rubner, M. F. *Thin Solid Films* **1994**, *244*, 985.
(67) Ferreira, M.; Cheung, J. H.; Rubner, M. F. *Thin Solid Films* **1994**, *244*, 806.
(68) Kotov, N. A.; Dékány, I.; Fendler, J. H. *J. Phys. Chem.* **1995**, *99*, 13065.
(69) Wu, A.; Yoo, D.; Lee, J.-K.; Rubner, M. F. *J. Am. Chem. Soc.* **1999**, *121*, 4883.
(70) Joly, S.; Kane, R.; Radzilowski, L.; Wang, T.; Wu, A.; Cohen, R. E.; Thomas, E. L.; Rubner, M. F. *Langmuir* **2000**, *16*, 1354.
(71) Harris, J. J.; Bruening, M. L. *Langmuir* **2000**, *16*, 2006.
(72) Mendelsohn, J. D.; Barrett, C. J.; Chan, V. V.; Pal, A. J.; Mayes, A. M.; Rubner, M. F. *Langmuir* **2000**, *16*, 5017.
(73) Shiratori, S. S.; Rubner, M. F. *Macromolecules* **2000**, *33*, 4213.
(74) Yoo, D.; Shiratori, S. S.; Rubner, M. F. *Macromolecules* **1998**, *31*, 4309.
(75) Blaakmeer, J.; Böhmer, M. R.; Stuart, C. M. A.; Fleer, G. J. *Macromolecules* **1990**, *23*, 2301.
(76) Ferreira, M.; Rubner, M. F. *Macromolecules* **1995**, *28*, 7107.
(77) Lvov, Y.; Decher, G.; Möhwald, H. *Langmuir* **1993**, *9*, 481.
(78) Böhmer, M. R.; Evers, O. A.; Scheutjens, J. M. H. M. *Macromolecules* **1990**, *23*, 2288.
(79) Kolarik, L.; Furlong, D. N.; Joy, H.; Struijk, C.; Rowe, R. *Langmuir* **1999**, *15*, 8265.
(80) Ho, P. K. H.; Friend, R. H. *Synth. Met.* **1999**, *102*, 1021.
(81) Steitz, R.; Leiner, V.; Siebrecht, R.; v. Klitzing, R. *Colloids Surf. A: Physicochem. Eng. Aspects* **2000**, *163*, 63.
(82) Lösche, M.; Schmitt, J.; Decher, G.; Bouwman, W. G.; Kjaer, K. *Macromolecules* **1998**, *31*, 8893.
(83) Decher, G.; Lvov, Y.; Schmitt, J. *Thin Solid Films* **1994**, *244*, 772.
(84) Tsuru, T.; Nakao, S.-i.; Kimura, S. *J. Membr. Sci.* **1995**, *108*, 269.

and co-workers showed that one polyelectrolyte layer deposited on an oppositely charged commercial reverse osmosis membrane provides selective transport of monovalent ions over divalent ions.[84−86] Deposition of multilayer polyelectrolyte films on porous supports differs from this procedure in that it forms a defect-free "skin" on a highly permeable support. The use of layered polyelectrolyte films also provides additional versatility in membrane formation, as mentioned above. Two recent studies showed that membranes consisting of polyelectrolyte multilayers exhibit monovalent/divalent ion-transport selectivities.[6,39]

This paper focuses on enhancing the ion-transport selectivity of layered polyelectrolyte membranes. Deposition of hybrid PSS/PAH/PAA membranes combined with cross-linking of PAA/PAH films yields average Cl^-/SO_4^{2-} selectivities as high as 360. Additionally, we utilized field-emission scanning electron microscopy (FESEM) and Fourier transform infrared external reflection spectroscopy (FTIR-ERS) to qualitatively investigate the chemistry behind these selectivity enhancements.

Experimental Section

Materials. Poly(allylamine hydrochloride) (Aldrich, M_w = 70 000), poly(sodium 4-styrenesulfonate) (Aldrich, M_w = 70 000), poly(acrylic acid) (Alfa Aesar, M_w = 90 000, 25 wt % solution), $MnCl_2$ (Acros), NaBr (Aldrich), NaCl (Spectrum), KCl (Baker), $MgCl_2$ (Spectrum), K_2SO_4 (CCI), $K_2Ni(CN)_4$ (Aldrich), and $K_3Fe(CN)_6$ (Mallinckrodt) were used as received. Porous alumina membrane filters (Whatman Anodisc, 0.02 μm surface pore diameter) were used as received except for cases where films were cross-linked by heating. In those cases, the polymeric support ring surrounding the alumina substrate was removed by heating at 400 °C for 18 h. This prevents the polymer ring from melting into the substrate pores during heat treatments. Martin and co-workers previously demonstrated the utility of porous alumina for forming and investigating ultrathin membranes.[87−89] Silicon (100, p-type) wafers were sputter coated with aluminum (∼200 nm) and used for ellipsometry measurements and reflectance FTIR spectra.

Synthesis of Polyelectrolyte Films. Prior to film deposition, aluminum-coated silicon wafers and porous alumina supports were UV/O_3 cleaned for 15 min (Boekel UV-Clean model 135500). Porous alumina supports were then placed in an O-ring holder that exposed only the top of the substrate to solutions in an effort to restrict deposition to the filtrate side of the alumina. Polyelectrolyte deposition began by immersion of the positively charged Anodisc or aluminum-coated slide in a polyanion solution: PSS (0.02 M, pH 2.1, 0.5 M $MnCl_2$) for 2 min or PAA (0.02 M, pH 4.5, 0.5 M NaCl) for 5 min. Polymer molarites are always given with respect to the repeating unit. The surface was rinsed for 1 min with deionized water (Milli-Q, 18.2 MΩ cm) after deposition of each polyelectrolyte layer. After being rinsed, the surface was immersed in a solution of PAH (0.02 M) for 5 min. Two solutions of PAH (pH 2.3, 0.5 M NaBr and pH 4.5, 0.5 M NaCl) were prepared. The former PAH solution was used for PSS/PAH films, while the latter was used for PAA/PAH films. Both solutions were used for hybrid films containing PSS, PAH, and PAA. Hybrid films were synthesized through deposition of a 5-bilayer PSS/PAH precursor film followed by deposition of a PAA layer or PAA/PAH bilayers. The PAH solution adjusted to pH 2.3 was used at the interface between PSS and PAA layers unless otherwise stated. After deposition of all layers, each film was dried with N_2 and stored at room temperature. After film deposition and drying, membranes and wafers to be cross-linked were placed in a flask that was then purged with N_2 for 15 min. The flask was slowly heated to the desired temperature (approximately 45-min ramping time) and then heated further for 2 h. All heating was done under a small flow of N_2.

Film Characterization. Ellipsometry measurements on aluminum-coated silicon wafers were made using a rotating analyzer ellipsometer (model M-44, J. A. Woollam) and WVASE32 software.[71] At least three separate areas on each sample were measured. Reflectance FTIR spectra of polyelectrolyte films on aluminum-coated silicon wafers were obtained using a Nicolet Magna-IR 560 spectrometer. A Hitachi S-4700 FESEM instrument (accelerating voltage of 6−8 kV) was used to image polyelectrolyte films deposited on porous alumina membranes, and samples were sputter-coated with ∼5 nm of Au prior to imaging.

Ion-Permeability Studies. The permeability apparatus consists of two glass cells (volumes of 90 mL) connected by an O-ring in the middle of a 2.5-cm-long neck. The membrane separates the feed and permeate cells of the apparatus with an exposed area of 1.7−2.0 cm^2. The polyelectrolyte films were exposed to the feed cell, which contained 0.1 F salt solutions of KCl, K_2SO_4, $K_2Ni(CN)_4$, $K_3Fe(CN)_6$, NaCl, $MgCl_2$, or KCl and $K_2Ni(CN)_4$. The receiving cell was filled with deionized water, and the ion concentration in this cell was monitored using a conductivity meter (Orion model 115). After an initial conductivity reading of the receiving cell, both sides were vigorously stirred, and the permeate conductivity was recorded every 10 minutes for 90 min. Normalized conductivities were calculated by dividing the receiving-phase conductivities by the final source-phase conductivity (dividing by the final source-phase conductivity rather than the initial source-phase conductivity changes the normalized conductivity value by less than 10%). Permeability experiments using K_2SO_4, $K_2Ni(CN)_4$, $MgCl_2$, $K_3Fe(CN)_6$, and KCl and $K_2Ni(CN)_4$ through hybrid films showed an average transfer of about 7, 8, 5, 10, and 5 mL of water, respectively, from the receiving phase to the source phase over the 90-min period. Between permeability experiments with different ions, both sides of the apparatus were rinsed and filled with deionized water. The cells were allowed to equilibrate with deionized water for an additional 20 min and then rinsed once more. Most membrane permeability experiments were run in the order KCl, K_2SO_4, $K_3Fe(CN)_6$, and KCl. Only those results from the first KCl run are reported.

The second KCl run was performed to test the integrity of the film. Most films show a change of less than 15% in Cl^- flux between the first and second trials. However, hybrid membranes with more than 1.5 bilayers of PAA/PAH showed 25−50% decreases in the second Cl^- flux. A decrease in Cl^- flux[39] might be due to $Fe(CN)_6^{3-}$ binding to the films, as we observed little decrease (<5%) in Cl^- flux during the final KCl run when $Fe(CN)_6^{3-}$ permeability was not measured. Pure and hybrid membranes heat-treated at 215 °C showed a 50% increase in Cl^- flux between the first and second trials. This might indicate conditioning of films that are highly cross-linked. Flux through these films is very low, in any case.

For a few types of membranes, cation transport was also measured. Initially, NaCl and $MgCl_2$ solutions were tested after the final KCl solution of the above-mentioned permeability experiments. However, in later experiments, we tested NaCl and $MgCl_2$ solutions before the $K_3Fe(CN)_6$ solution to avoid a possible influence of $Fe(CN)_6^{3-}$ adsorption on cation transport. These experiments reveal that this change in order affects the Na^+/Mg^{2+} selectivity by <30%. Additional permeability experiments were performed with a mixed salt solution of KCl and $K_2Ni(CN)_4$. By substituting $K_2Ni(CN)_4$ for K_2SO_4 in a mixed salt solution, we were able to employ graphite-furnace atomic absorption spectrophotometry (AAS) (Hitachi Z-9000) to detect $Ni(CN)_4^{2-}$. The KCl concentration could still

(85) Tsuru, T.; Urairi, M.; Nakao, S.; Kimura, S. *Desalination* **1991**, *81*, 219.
(86) Urairi, M.; Tsuru, T.; Nakao, S.; Kimura, S. *J. Membr. Sci.* **1992**, *70*, 153.
(87) Chen, W. J.; Aranda, P.; Martin, C. R. *J. Membr. Sci.* **1995**, *107*, 199.
(88) Chen, W. J.; Martin, C. R. *J. Membr. Sci.* **1995**, *104*, 101.
(89) Liu, C.; Martin, C. R. *Nature* **1991**, *352*, 50.

Table 1. Ellipsometric Thicknesses of PAA/PAH Films and Anion Fluxes (mol cm^{-2} s^{-1}) through Bare Porous Alumina and Alumina Coated with PAA/PAH Films that were Partially Cross-Linked at Different Temperatures

film composition	T^a/°C	thickness^b/Å	Cl^- flux/10^{-8}	SO_4^{2-} flux/10^{-8}	Cl^-/SO_4^{2-} ^{c}
bare membrane	–	–	5.3 ± 3%	3.0 ± 5%	1.7 ± 4%
bare membrane^d	400	–	5.2 ± 10%	3.5 ± 7%	1.5 ± 2%
4 PAA/PAH	–	316 ± 15	–	–	–
4.5 PAA/PAH	–	390 ± 20	1.3 ± 6%	0.29 ± 7%	4.5 ± 10%
4.5 PAA/PAH	105	–	1.2 ± 15%	0.13 ± 35%	9.5 ± 25%
4.5 PAA/PAH	110	–	0.96 ± 10%	0.092 ± 25%	11 ± 20%
4.5 PAA/PAH	115	360 ± 6	0.68 ± 25%	0.043 ± 60%	20 ± 45%
4.5 PAA/PAH	130	340 ± 20	0.17 ± 55%	0.026 ± 60%	7 ± 40%
4.5 PAA/PAH	215	300 ± 13	0.0041 ± 25%	0.0016 ± 55%	3.1 ± 55%
5 PAA/PAH	–	–	1.1 ± 10%	1.1 ± 10%	0.97 ± 10%
5 PAA/PAH	115	–	0.56 ± 40%	0.97 ± 45%	0.60 ± 25%

^{a} Temperature at which membranes were heated for 2 h to partially cross-link films. ^{b} Thicknesses were measured with films deposited on Al-coated Si wafers. ^{c} Cl^-/SO_4^{2-} ratios were calculated from the average of selectivities of different membranes and not from the average flux values. This results in a lower standard deviation and a slightly different average value. ^{d} For cross-linked PAA/PAH films, alumina was heated at 400 °C prior to film deposition to remove the polymer support ring. These data are for bare alumina heated at 400 °C.

be determined using conductivity measurements with a small correction for the $Ni(CN)_4^{2-}$ concentration.

Each type of polyelectrolyte membrane was tested with three or more different membranes unless otherwise noted. Flux values were calculated from calibration curves of conductivity versus concentration because the relationship between concentration and measured conductivity is nonlinear. Because the conductivity of the receiving-phase solution was very low in experiments with $K_3Fe(CN)_6$, we also determined $Fe(CN)_6^{3-}$ concentrations using graphite-furnace AAS in a few cases. These determinations agreed to within at least 60% of concentrations determined using conductivity measurements. This agreement is acceptable considering the very low conductivity values of these solutions. However, it does demonstrate that the $Fe(CN)_6^{3-}$ flux values could contain as much as 60% error.

Results and Discussion

Anion Permeability through Cross-Linked PAA/PAH Membranes. Our previous studies showed that ultrathin, layered polyelectrolyte films on porous alumina exhibit Cl^-/SO_4^{2-} selectivities ranging from 5 to 9.[39,90,91] The selectivity of these membranes might be limited by film swelling in the presence of water.[37,71,81] In an effort to limit swelling, we prepared PAA/PAH membranes that were cross-linked through heat-induced amide formation from the carboxylate groups of PAA and the ammonium groups of PAH. FTIR spectra of films on alumina show that the amount of amide formation increases with temperature until 215 °C, at which point amidation is virtually quantitative.[92,93] Temperatures as low as 115 °C induce some amide bond formation, as suggested by a 20% decrease in the absorbance of $-COO^-$ peaks (1570 and 1400 cm^{-1}) after heating. Table 1 presents thicknesses of 4.5-bilayer PAA/PAH films after they were heated at various temperatures. As more amide bonds form during heating, water is lost, and the films become more compact. Heating might also drive adsorbed water from the films.

The deposition of PAA/PAH films on porous alumina results in ultrathin composite membranes such as that shown in Figure 1 (C and D). The top view shows that the highly textured polyelectrolyte film covers the surface (image C), while the cross-sectional view shows that the film does not fill the substrate pores (image D). Images of bare alumina (A and B) are given for comparison. The figure shows a PAA/PAH-coated substrate that was partially cross-linked at 115 °C, but unheated films give similar images.[72]

The anion flux through 4.5-bilayer PAA/PAH membranes depends strongly on cross-linking temperature, as shown in Table 1. As the cross-linking within the films increases, the transport of both Cl^- and SO_4^{2-} ions through these films decreases. Low degrees of cross-linking decrease the SO_4^{2-} flux more than the Cl^- flux, resulting in increased Cl^-/SO_4^{2-} selectivity values. A peak Cl^-/SO_4^{2-} selectivity of ~20 occurs for films cross-linked at 115 °C. This is a ~4-fold increase in selectivity over unheated films. Heating PAA/PAH films at temperatures above 115 °C continues to cause the flux of both anions to decrease, but the Cl^- flux begins to decrease more rapidly than the SO_4^{2-} flux. Thus, a decrease in the Cl^-/SO_4^{2-} selectivity occurs when these membranes are cross-linked at high temperatures.

We also deposited an additional PAH layer on an unheated 4.5-bilayer PAA/PAH film to change the surface charge from negative to positive.[37] Deposition of a PAH layer increases the SO_4^{2-} flux 4-fold and decreases the Cl^- flux by 15%. Thus, the presence of a terminating PAH layer eliminates the selectivity between Cl^- and SO_4^{2-}, as shown in Table 1. PAA/PAH membranes that are cross-linked at 115 °C show a Cl^-/SO_4^{2-} selectivity reversal (from 20 to 0.6) upon going from a 4.5-bilayer to a 5-bilayer PAA/PAH film. Previous electrochemical studies also showed that transport of multiply charged ions depends on the surface charge of layered polyelectrolyte films.[94–96]

The decrease or reversal of the Cl^-/SO_4^{2-} selectivity upon deposition of a cationic PAH layer on 4.5-bilayer

(90) Tieke and co-workers reported Cl^-/SO_4^{2-} selectivity values of 17 for 5-bilayer PAH/PSS films on porous polymeric supports. The higher selectivities might result from different deposition conditions.

(91) In our previous paper (ref 39), we assumed a linear relationship between conductivity and concentration rather than using calibration curves. For comparison with our current results, we have recalculated all flux and selectivity values in that paper using calibration curves. Use of the calibration curves resulted in average flux decreases of 25% for Cl^-, 45% for SO_4^{2-}, and 50% for $Fe(CN)_6^{3-}$ for both 5-bilayer PAH/PSS and 5-bilayer PAH/PAA membranes.

(92) Harris, J. J.; DeRose, P. M.; Bruening, M. L. *J. Am. Chem. Soc.* **1999**, *121*, 1978.

(93) Dai, J.; Sullivan, D. M.; Bruening, M. L. *Ind. Eng. Chem. Res.* **2000**, *39*, 3528.

(94) Farhat, T. R.; Schlenoff, J. B. *Langmuir* **2001**, *17*, 1184.

(95) Pardo-Yissar, V.; Katz, E.; Lioubashevski, O.; Willner, I. *Langmuir* **2001**, *17*, 1110.

(96) Lvov, Y. In *Protein Architecture—Interfacing Molecular Assemblies and Immobilization Biotechnology*; Lvov, Y., Möhwald, H., Eds.; Marcel Dekker: New York, 2000; p 135.

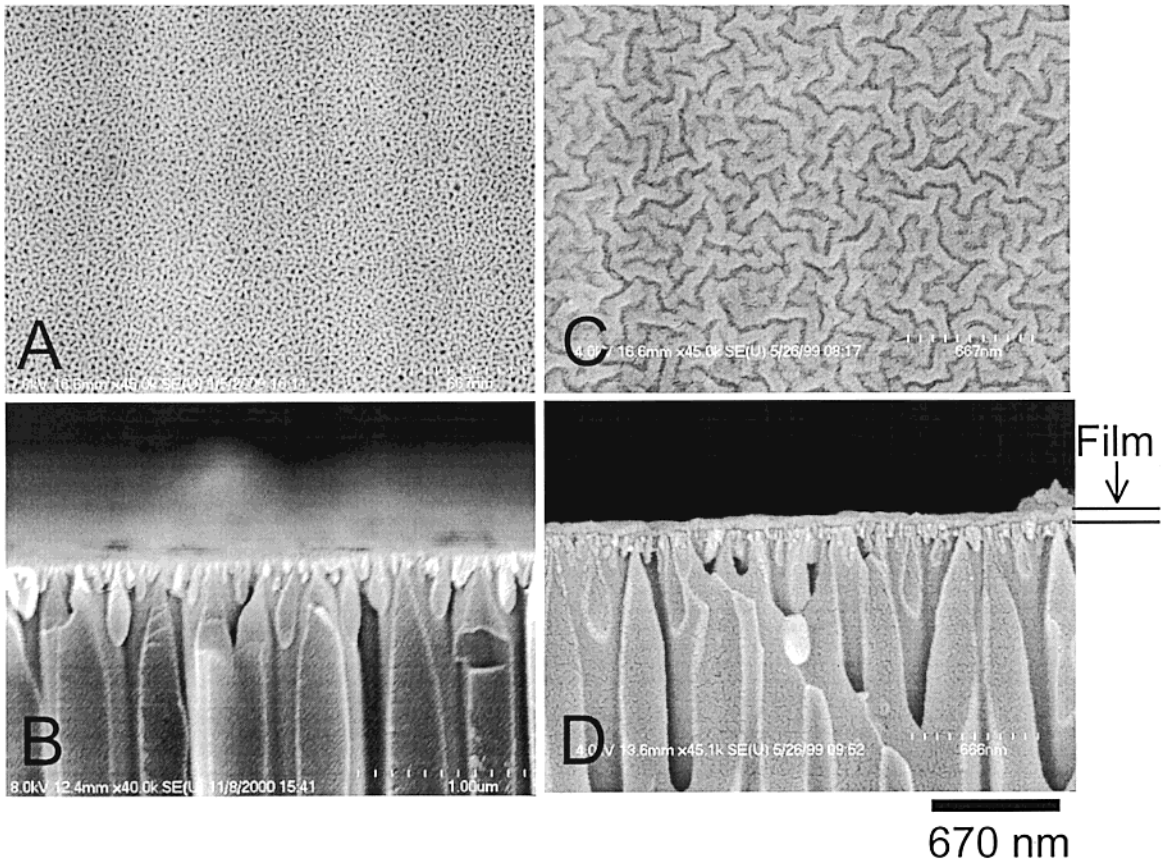

Figure 1. FESEM images of (A) the top and (B) a cross section of a bare porous alumina membrane and similar images of (C) the top and (D) a cross section of an alumina membrane coated with a 4.5-bilayer PAA/PAH film that was heated at 115 °C. Samples were coated with ~5 nm of gold prior to imaging. The scale bar is common to all images.

PAA/PAH films implies that Donnan exclusion at the membrane surface is the major factor behind selectivity. The increase in Cl^-/SO_4^{2-} selectivity upon heating a 4.5-bilayer PAA/PAH film at 115 °C further suggests that cross-linking enhances Donnan exclusion. Cross-linking might decrease swelling at the surface and increase surface charge density, thus enhancing exclusion of multivalent ions. Although heating at higher temperatures should further decrease the swelling, conversion of $-COO^-$ groups to amides might reduce the surface charge density at high degrees of cross-linking. This would explain why the Cl^-/SO_4^{2-} selectivity decreases for films cross-linked at temperatures higher than 115 °C. Decreased swelling at higher degrees of cross-linking should also result in slower ion diffusion, which is consistent with the low fluxes that occur through highly cross-linked films.

Synthesis of Hybrid PSS/PAH/PAA Films. PAA/PAH films are attractive materials because their properties can be modified by heat-induced cross-linking. However, the Cl^- flux through cross-linked and non-cross-linked PAA/PAH films is at least three times less than that through unheated 4.5-bilayer PSS/PAH membranes. With this in mind, we began preparing multilayer PSS/PAH films that could be capped with one to three bilayers of PAA/PAH. A few PAA/PAH layers could provide selectivity with a minimal diminution of flux.

The reflectance FTIR spectra in Figure 2 show the presence of all three types of polyelectrolytes after deposition of each additional PAA or PAH layer on the

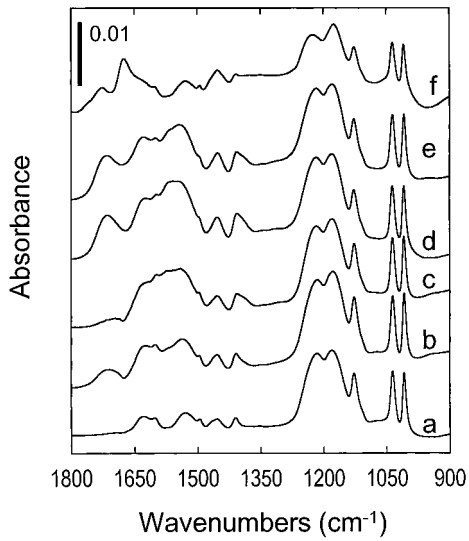

Figure 2. Reflectance FTIR spectra of (a) a 5-bilayer PSS/PAH film and 5-bilayer PSS/PAH films coated with (b) 1 layer of PAA, (c) 1 bilayer of PAA/PAH, and (d) 1.5 bilayers of PAA/PAH. Spectra e and f are those of 5-bilayer PSS/PAH films coated with 1.5 bilayers of PAA/PAH and subsequently cross-linked at 115 °C and 215 °C, respectively.

PSS/PAH precursor film. The spectrum of a 5-bilayer PSS/PAH film (spectrum a) shows strong sulfonate absorbances at 1220, 1175, 1035, and 1005 cm^{-1} [97,98] and

(97) Caruso, F.; Furlong, D. N.; Ariga, K.; Ichinose, I.; Kunitake, T. *Langmuir* **1998**, *14*, 4559.
(98) Wang, F.; Li, J.; Chen, T.; Xu, J. *Polymer* **1999**, *40*, 795.

Table 2. Ellipsometric Thicknesses of Pure PSS/PAH and Hybrid PSS/PAH/PAA Films and Anion Fluxes (mol cm^{-2} s^{-1}) through Pure PSS/PAH, Hybrid PSS/PAH/PAA, and Heated PSS/PAH/PAA Films

film composition	T/°C[a]	thickness/Å[b]	Cl^- flux/10^{-8}	SO_4^{2-} flux/10^{-9}	$Fe(CN)_6^{3-}$ flux/10^{-11}	Cl^-/SO_4^{2-}[c]	$Cl^-/Fe(CN)_6^{3-}/10^3$[c]
4.5 PSS/PAH	–	170 ± 6	4.3 ± 8%	8.5± 15%	5.7 ± 70%	5.1 ± 15%	1.0 ± 65%
4.5 PSS/PAH	115	–	4.0 ± 4%	4.0± 15%	3.1 ± 20%	10 ± 15%	1.3 ± 20%
5 PSS/PAH	–	190 ± 8	–	–	–	–	–
5 PSS/PAH[d]	–	190 ± 18	3.5 ± 9%	9.6 ± 25%	8.1 ± 95%	3.8 ± 20%	0.76 ± 70%
5 PSS/PAH + 1 layer PAA	–	214 ± 14	4.0 ± 8%	1.6 ± 4%	3.6 ± 30%	25 ± 5%	1.2 ± 30%
5 PSS/PAH + 1 layer PAA	115	–	3.4 ± 4%	1.0 ± 20%	2.6 ± 120%	35 ± 20%	4.7± 120%
5 PSS/PAH + 1 layer PAA[e]	–	210 ± 9	3.5 ± 2%	1.4 ± 50%	4.1 ± 35%	30 ± 55%	0.94 ± 40%
5 PSS/PAH + 1 PAA/PAH	–	225 ± 5	–	–	–	–	–
5 PSS/PAH + 1 PAA/PAH[e]	–	220 ± 14	–	–	–	–	–
5 PSS/PAH + 1 PAA/PAH	115	–	3.0 ± 4%	7.7 ± 15%	3.2 ± 75%	4.0 ± 10%	1.4 ± 60%
5 PSS/PAH + 1.5 PAA/PAH	–	270 ± 13	3.1 ± 7%	0.47 ± 25%	1.2 ± 40%	70 ± 20%	3.0 ± 35%
5 PSS/PAH + 1.5 PAA/PAH	115	–	2.4 ± 20%	0.18 ± 65%	0.87 ± 45%	160 ± 30%	3.8 ± 70%
5 PSS/PAH + 1.5 PAA/PAH	120	–	1.7 ± 20%	0.10 ± 10%	1.24 ± 10%	160 ± 15%	1.4 ± 30%
5 PSS/PAH + 1.5 PAA/PAH	215	–	0.14 ± 35%	0.025 ± 95%	1.2 ± 50%	110 ± 90%	0.16 ± 60%
5 PSS/PAH + 1.5 PAA/PAH[e]	–	270 ± 11	2.8 ± 10%	0.25 ± 35%	1.2 ± 30%	120 ± 25%	2.5 ± 30%
5 PSS/PAH + 1.5 PAA/PAH[e]	115	–	2.6 ± 10%	0.23 ± 30%	1.7 ± 20%	120 ± 30%	1.5 ± 20%
5 PSS/PAH + 2.5 PAA/PAH	–	410 ± 22	2.3 ± 15%	0.25 ± 70%	1.2 ± 50%	120 ± 40%	2.1 ± 30%
5 PSS/PAH + 2.5 PAA/PAH	115	–	1.5 ± 30%	0.24 ± 75%	0.46 ± 115%	240 ± 120%	13 ± 100%
5 PSS/PAH + 2.5 PAA/PAH[e]	–	390 ± 30	2.4 ± 10%	0.20 ± 50%	0.83 ± 20%	150 ± 45%	3.0 ± 25%
5 PSS/PAH + 2.5 PAA/PAH[e]	115	–	2.3 ± 8%	0.10 ± 85%	2.3 ± 65%	360 ± 70%	1.3 ± 60%
5 PSS/PAH + 3 PAA/PAH[e]	–	460 ± 11	3.0 ± 15%	13 ± 10%	5.7 ± 10%	2.2 ± 5%	0.52 ± 20%

[a] Temperature at which membranes were heated for 2 h to partially cross-link films. [b] Thicknesses were measured with films deposited on Al-coated Si wafers. [c] Selectivity ratios were calculated from the average of selectivities of different membranes and not from the average flux values. This results in a lower standard deviation and a slightly different average value. [d] The top layer of PAH was deposited at a pH of 4.5 rather than 2.3. [e] The PAH layer between PSS and PAA was deposited at a pH of 4.5 rather than 2.3.

adsorption bands due to symmetric and antisymmetric $-NH_3^+$ deformations and aromatic ring modes between 1625 and 1400 cm^{-1}.[97,99] After deposition of one layer of PAA on the base PSS/PAH film (spectrum b), the −COOH carbonyl peak appears at ∼1710 cm^{-1}, and carboxylate peaks around 1570 and 1400 cm^{-1} also affect the spectrum. After 1.5 bilayers of PAA/PAH are deposited (spectrum d), peaks due to PAA become more obvious. The sulfonate peaks remain in the spectrum, showing the stability of the underlying layers during PAA/PAH deposition. Spectrum c indicates that some −COOH groups in the first adsorbed layer of PAA are converted to $-COO^-$ upon deposition of PAH. When the weak polyelectrolyte PAA is approached by a polycation, more deprotonation of the acid groups can occur.[73,75,78]

Table 2 gives the ellipsometric thicknesses of hybrid films as a function of the number of bilayers. The precursor 5-bilayer PSS/PAH film thickness of ∼190 Å agrees with previously reported values.[39,100] Increases in film thickness due to PAA/PAH growth on the PSS/PAH film are not linear with the number of layers deposited because of a change in deposition pH and the polyelectrolyte deposited.[77,73] A PAA layer deposited on four bilayers of PAA/PAH has a measured thickness of ∼70 Å, whereas a PAA layer deposited on five bilayers of PSS/PAH has a measured thickness of ∼25 Å.[101]

Heating of hybrid coatings should produce films with compact, cross-linked surfaces. Reflectance FTIR spectra verify cross-linking between PAA and PAH surface layers in hybrid films just as in the case of films composed only of PAA/PAH layers. After the samples are heated at 115 °C, a small decrease in the intensity of $-COO^-$ bands (1570 and 1400 cm^{-1}) occurs (spectrum e, Figure 2), whereas after they are heated at 215 °C, the IR spectrum shows almost complete conversion of carboxylate groups to amides (a strong amide peak appears at 1670 cm^{-1}) (spectrum f, Figure 2). The unvarying absorbances due to PSS indicate that no reaction between PSS and PAH layers occurs as a result of heating at 115 °C. However, we do observe a small decrease in sulfonate absorbances after heating at 215 °C.

Anion Permeability through Hybrid PSS/PAH/PAA Membranes. Membranes consisting of a 5-bilayer PSS/PAH precursor film and 0.5−2.5 bilayers of PAA/PAH show dramatic increases in selectivity over both 4.5-bilayer PSS/PAH and 4.5-bilayer PAA/PAH membranes. Table 2 contains anion fluxes through pure PSS/PAH films and PSS/PAH films capped with 0.5−3 PAA/PAH bilayers. The Cl^- flux through unheated hybrid films increases by 70−200% over that of a film composed only of 4.5 bilayers of PAA/PAH. Thus, the idea of increasing Cl^- flux by using a more permeable supporting layer is feasible. In contrast, the SO_4^{2-} flux through 5-bilayer PSS/PAH + 2.5-bilayer PAA/PAH films is <10% of the flux through 4.5-bilayer PAA/PAH films. The combination of high Cl^- and low SO_4^{2-} fluxes increases selectivity up to 30-fold over pure PAA/PAH films. The highest $Cl^-/Fe(CN)_6^{3-}$ selectivity for an unheated film is ∼3000, as shown in Table 2. As with Cl^-/SO_4^{2-} selectivities, this 9-fold increase over previously reported selectivities for 5-bilayer PAH/PAA membranes occurs as a result of both higher Cl^- and lower $Fe(CN)_6^{3-}$ permeabilities.[39,91]

Increased selectivities suggest that deposition of PAA on a PSS/PAH film yields a different surface structure than does deposition of PAA on pure PAA/PAH films. SEM images confirm that the surfaces of hybrid films are different from those of pure films (Figure 1C), as images of hybrid films show no distinct surface texture. The high selectivities among anions with different charges suggest that the PAA layer on hybrid films contains a higher charge density than does the top PAA layer on pure PAA/PAH films. Higher charge density

(99) Lin-Vien, D.; Colthup, N. B.; Fateley, W. G.; Grasselli, J. G. *The Handbook of Infrared and Raman Characteristic Frequencies of Organic Molecules*; Academic Press: New York, 1991.

(100) Sukhorukov, G. B.; Möhwald, H.; Decher, G.; Lvov, Y. *Thin Solid Films* **1996**, *284−285*, 220.

(101) The PAH layer at the interface between PSS/PAH and PAA/PAH films was deposited at a pH of 4.5.

would lead to greater selectivity as a result of Donnan exclusion.

We also evaluated the effect of changing the deposition pH of the PAH layer at the interface between PSS/PAH and PAA/PAH. To do this, we prepared films composed of 4.5 bilayers of PSS/PAH (deposition pH of 2.1/2.3) with both the following PAH layer and subsequent PAA/PAH layers deposited at pH 4.5. The addition of one layer of PAA to the PSS/PAH base layer showed no marked difference in anion selectivities compared to standard 5-bilayer PSS/PAH films (interfacial PAH layer deposited at pH 2.3) capped with a layer of PAA. An additional PAH/PAA bilayer, however, increased the Cl^-/SO_4^{2-} selectivity by 70% compared to standard 5-bilayer PSS/PAH + 1.5-bilayer PAA/PAH films. Addition of another PAH/PAA bilayer gives a Cl^-/SO_4^{2-} selectivity of around 150 for films with the modified interfacial layer. This selectivity, however, is not significantly higher than that of 5-bilayer PSS/PAH + 2.5 PAA/PAH films with the interfacial PAH layer deposited at pH 2.3.

Table 2 also displays the thicknesses of hybrid PSS/PAH/PAA films where the interfacial PAH layer was deposited at both pH 2.3 and pH 4.5. Films deposited with the same number of bilayers and a different interfacial PAH deposition pH showed no marked differences in thickness. Small structural differences in these two types of films apparently do not have a large effect on thickness.

As for pure PAA/PAH membranes, termination of hybrid films with PAH rather than PAA results in dramatic changes in multivalent anion fluxes. Adding a layer of PAH to a 5-bilayer PSS/PAH + 2.5-bilayer PAA/PAH[101] unheated membrane increases the SO_4^{2-} flux ~65-fold and the $Fe(CN)_6^{3-}$ flux ~7-fold, thus confirming the strong influence of Donnan exclusion.

Anion Permeability through Cross-Linked PSS/PAH/PAA Membranes. As with pure PAA/PAH films, heating of hybrid polyelectrolyte membranes (interfacial PAH layer deposited at pH 2.3) increases the Cl^-/SO_4^{2-} selectivity to peak levels at cross-linking temperatures around 115 °C, whereas heating at 215 °C causes the selectivity to decrease. Table 2 gives anion fluxes through 5-bilayer PSS/PAH + 1.5-bilayer PAA/PAH films that were heated at several temperatures. After 5-bilayer PSS/PAH + 1.5-bilayer PAA/PAH films were cross-linked at 115 °C, Cl^-/SO_4^{2-} selectivity increased from 70 to 160. Figure 3 compares anion fluxes through a 5-bilayer PSS/PAH precursor film and through 5-bilayer PSS/PAH + 1.5-bilayer PAA/PAH membranes before and after cross-linking. Each subsequent modification increases the Cl^-/SO_4^{2-} selectivity while slightly decreasing the Cl^- flux. We also heated a 5-bilayer PSS/PAH + 2.5-bilayer PAA/PAH film at 115 °C in an attempt to increase selectivity to even higher values. However, data for these heated films were not reproducible enough to make a good comparison.

As for pure PAA/PAH films, with increasing cross-linking temperature, the number of $-COO^-$ groups that form amide bonds probably increases, and the selectivity eventually decreases as a result of a reduction in charge density. Heating a 5-bilayer PSS/PAH + 1.5-bilayer PAA/PAH film at 215 °C still yields a Cl^-/SO_4^{2-} selectivity of ~110, however. In comparison, a 4.5-bilayer PAA/PAH membrane heated at 215 °C has a Cl^-/SO_4^{2-} selectivity value of only 3. The flux values show that this difference in selectivity is due mainly to higher Cl^- fluxes through the more permeable hybrid film.

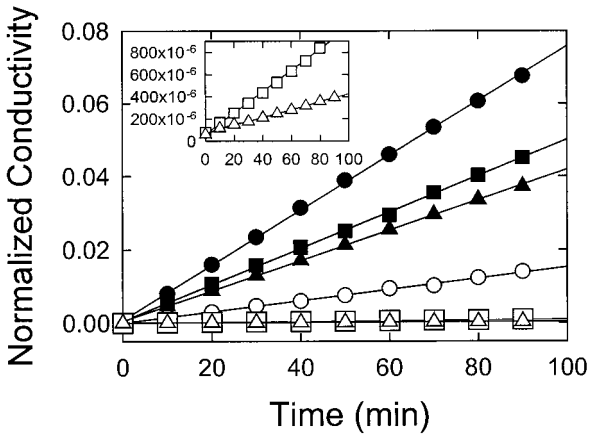

Figure 3. Plot of normalized receiving-phase conductivity as a function of time when the source phase (0.1 F salt) was separated from the receiving phase by a 5-bilayer PSS/PAH film (circles), a 5-bilayer PSS/PAH + 1.5-bilayer PAA/PAH film (squares), and a 5-bilayer PSS/PAH + 1.5-bilayer PAA/PAH film heated at 115 °C (triangles). Different colors represent different salts: black, KCl and white, K_2SO_4. The inset expands the conductivity scale for SO_4^{2-} transport through hybrid membranes. (The PAH layer between PSS and PAA was deposited at pH 2.3.)

Heating 5-bilayer PSS/PAH + 1.5-bilayer PAA/PAH films prepared with the interfacial PAH layer deposited at pH 4.5 did not greatly affect anion transport, but these films are already very selective. The fluxes of all anions remained similar to those of unheated films, suggesting that the charge density of these films does not change greatly upon heating at 115 °C. In the case of 5-bilayer PSS/PAH + 2.5-bilayer PAA/PAH films prepared with the interfacial PAH layer deposited at pH 4.5, data for heated films show too much scatter to make any conclusion about the effect of cross-linking. The $Fe(CN)_6^{3-}$ fluxes through most hybrid films are extremely low, and there is no clear correlation between flux and either the deposition pH of the interfacial PAH or heating.

Cation Permeability through Hybrid PSS/PAH/PAA Membranes. In an effort to increase our understanding of how surface charge affects selectivity, we tested Na^+ and Mg^{2+} transport through 5-bilayer PSS/PAH + 2.5-bilayer PAA/PAH and 5-bilayer PSS/PAH + 3-bilayer PAA/PAH films. Flux values (Table 3) show Na^+/Mg^{2+} selectivities of 40−80 for 5-bilayer PSS/PAH + 2.5-bilayer PAA/PAH films. These values indicate that, unlike Cl^-/SO_4^{2-} selectivity, Na^+/Mg^{2+} selectivity is quite high for films capped with a layer whose charge is opposite to that of the transporting species. Tieke and co-workers also demonstrated that polyanion-terminated membranes can give good cation selectivities. They showed that 5, 10, and 60 bilayers of PAH/PSS on a polymer support give Na^+/Mg^{2+} selectivities of 31, 36, and 113, respectively.[6] In an effort to increase the cation selectivity of hybrid films, we capped these coatings with an additional layer of PAH. This additional layer of PAH increased the Na^+/Mg^{2+} selectivity to only ~140. We speculate that the high cation selectivities of these films, irrespective of the capping layer, might occur as a result

Table 3. Cation Fluxes (mol cm^{-2} s^{-1}) through Hybrid PSS/PAH/PAA Films

film composition	Na^+ flux/10^{-8}	Mg^{2+} flux/10^{-10}	Na^+/Mg^{2+} [a]
5 PSS/PAH + 2.5 PAA/PAH	1.7 ± 20%	3.8 ± 40%	50 ± 30%
5 PSS/PAH + 2.5 PAA/PAH[b]	1.6 ± 20%	2.0 ± 35%	80 ± 15%
5 PSS/PAH + 2.5 PAA/PAH[b,c]	1.7 ± 20%	4.3 ± 20%	40 ± 6%
5 PSS/PAH + 3 PAA/PAH[b]	2.6 ± 3%	1.9 ± 9%	140 ± 6%

[a] Average Na^+/Mg^{2+} values were calculated from the average of selectivities of each membrane type. This results in a lower standard deviation. [b] The PAH layer between PSS and PAA was deposited at a pH of 4.5 rather than 2.3. [c] These membranes were heated at 115 °C for 2 h as described in the Experimental Section.

Table 4. $Ni(CN)_4^{2-}$ and Cl^- Fluxes (mol cm^{-2} s^{-1}) through 5-Bilayer PSS/PAH + 2.5-Bilayer PAA/PAH Films[a,b]

salt solution	Cl^- flux/10^{-8}	$Ni(CN)_4^{2-}$ flux/10^{-8}	$Ni(CN)_4^{2-}$ flux/10^{-8} [d]
$Cl^-/Ni(CN)_4^{2-}$	2.6 [c]	–	0.014
$Ni(CN)_4^{2-}$	–	0.011	0.012
Cl^-	2.4	–	–

[a] The PAH layer between PSS and PAA was deposited at a pH of 4.5 rather than 2.3. [b] Fluxes were calculated from the average of two measurements. Differences between the two measurements were less than 30%. [c] Flux was calculated using conductivity after making a small correction for conductivity due to $Ni(CN)_4^{2-}$. [d] Flux was calculated from atomic absorption measurements.

of adsorption of the divalent cation,[102,103] which yields a positively charged membrane surface and increased Donnan exclusion. The adsorption of cations might be more favorable than that of anions, which would explain the relatively small increase in cation selectivity due to capping with a polycation.

Permeability of Mixtures through Hybrid PSS/PAH/PAA Membranes. The permeability experiments described up to this point were run with solutions containing a single salt. Actual separations will occur from mixtures, so we began evaluating transport from solutions containing both Cl^- and $Ni(CN)_4^{2-}$. Unfortunately, conductivity measurements alone cannot distinguish between two ionic species, so we utilized $K_2Ni(CN)_4$ as a substitute for K_2SO_4 so that $Ni(CN)_4^{2-}$ transport could be detected using atomic absorption spectrophotometry. Table 4 gives the Cl^- and $Ni(CN)_4^{2-}$ fluxes through 5-bilayer PSS/PAH + 2.5-bilayer PAA/PAH[101] films from single electrolyte and mixed electrolyte solutions. A comparison of Table 4 and Table 2 shows that the permeability of $Ni(CN)_4^{2-}$ through 5-bilayer PSS/PAH + 2.5-bilayer PAA/PAH[101] films is similar to that of SO_4^{2-}. Both the Cl^- and $Ni(CN)_4^{2-}$ fluxes are similar in mixed electrolyte and single-salt solutions, suggesting that single-salt experiments provide a good initial indication of membrane selectivity. These results also suggest that osmotic flow has little effect on ion transport, because the flow of water between source and receiving phase is about 5 mL for the mixed $Cl^-/Ni(CN)_4^{2-}$ solution and <2 mL for a 0.1 M KCl solution.

Conclusions

Deposition of PAA/PAH bilayers on PSS/PAH films on porous alumina substrates creates highly selective ion-transport membranes with minimal thicknesses. The PSS/PAH precursor film provides relatively little resistance to mass transport, while the PAA/PAH surface layers discriminate against transport of multiply charged ions. Furthermore, heat-induced cross-linking of PAA/PAH surface bilayers enhances the overall average Cl^-/SO_4^{2-} selectivity to average values as high as 360. These values are almost 2 orders of magnitude higher than those previously reported for 5-bilayer PAH/PSS or 5-bilayer PAH/PAA films on porous alumina.[39,91] The Cl^- flux through hybrid films is also up to three times higher than that through pure PAA/PAH films. Changing the surface charge from negative to positive dramatically reduces, and in some cases reverses, Cl^-/SO_4^{2-} selectivity for both pure and hybrid films, suggesting that Donnan exclusion at the surface is the primary factor behind selective anion transport. In contrast, both polyanion- and polycation-terminated films show selectivity among cations. Experiments with mixed solutions containing Cl^- and $Ni(CN)_4^{2-}$ ions showed that single-salt permeability measurements effectively represent transport from mixed solutions. Thus, hybrid polyelectrolyte membranes can provide highly selective barriers for water purification processes.

Acknowledgment. We acknowledge partial financial support from the Division of Chemical Sciences, Office of Energy Research, U.S. Department of Energy; Michigan State University; and the W. M. Keck Microfabrication Facility.

CM010166E

(102) Peeters, J. M. M.; Mulder, M. H. V.; Strathmann, H. *Colloids Surf. A: Physicochem. Eng. Aspects* **1999**, *150*, 247.
(103) Takagi, R.; Nakagaki, M. *J. Membr. Sci.* **1992**, *71*, 189.